Mesoporous silica matrices derived from sol-gel process assisted by low power ultrasonic activation

Cecilia Savii[1,*], László Almásy[2,3], Claudia Ionescu[4], Noémi Kinga Székely[5], Corina Enache[1], Mihaela Popovici[6], Ioan Sora[7], Dan Nicoara[7], George Gustav Savii[7], Dana Susan Resiga[8], Jan Subrt[9], Václav Štengl[9]

[1]*Institute of Chemistry Timisoara of Romanian Academy, Bv. Mihai Viteazul Nr. 24, 300223, Romania*
[2]*Laboratory for Neutron Scattering, PSI and ETH Zürich, CH-5232 Villigen, Switzerland*
[3]*Adolphe Merkle Institute, University of Fribourg, CH-1700 Fribourg, Switzerland*
[4]*Department of Physics, University of Warwick, Coventry, CV4 7AL, United Kingdom*
[5]*Research Institute for Solid State Physics and Optics, POB 49, 1525-Budapest, Hungary*
[6]*IMEC, Kapeldreef 75, 3001 Heverlee, Belgium*
[7]*Faculty de Electrotechnics, University "Politehnica" Timisoara, Bv. Parvan nr. 1, Romania*
[8]*Faculty of Physics, West University of Timisoara, Bv. Parvan nr. 4, Timisoara, Romania*
[9]*Department of Solid State Chemistry, Institute of Inorganic Chemistry, Academy of Sciences of the Czech Republic, 250 68 Řež, Czech Republic*

Received 23 October 2008; received in revised form 11 March 2009; accepted April 8 2009

Abstract

The present work contributes to elucidating the differences between silica gels obtained by low doses ultrasonic activation, and those obtained by the conventional method, termed as classical sol gel. Silica matrices were produced by sol-gel synthesis process, assisted and non-assisted by an ultrasonic field, and subsequently characterized by various methods. Nitrogen adsorption and small-angle neutron scattering (SANS) measurements provided texture and microstructure of the dried gels. The adsorption results show that the sample sonicated for 2 hours presents the most ordered microstructure, characterized by pore shape close to spherical and the narrowest size distribution – about 90 % of the pores for this sample fall into the mesopore range (2–50 nm). SANS data reveal the formation of primary structural units of sizes around 1.5–2 nm which are small linear or branched polymeric species of roughly spherical shape and with rough surface. They are generated in the very early stage of sol gel process, as a result of hydrolysis and condensation reactions. The aggregated primary units form the secondary porous structure which can be described as a rough surface with fractal dimension above 2. The best porosity characteristics were obtained for the sample activated for 2 hours, indicating the optimal doses of sonication in the present conditions. Our results demonstrate the possibility of tailoring the pore size distribution using a low power ultrasonic bath.

Keywords*: mesoporous silica matrix, sol-gel, sonication, SANS, fractal structure, specific surface area*

I. Introduction

The sol-gel process has been developed over the last two decades leading to new materials in various areas [1–4]. The use of „soft chemistry" for solid preparation is now-days strongly connected to polymer science. The physical properties of the highly cross linked polymer gels are controlled by the mechanism of the reaction used to build the chains of the resulting macromolecules [5]. The texture of the obtained solid, described in terms of macroscopic properties (specific surface area, porosity, density etc.) is highly dependent on the experimental conditions [5–7]. It is important to point out the flexible processability inherent in the formation of the sol. The sol is a viscous liquid that allows various structures to be obtained: films, fibres as well as matrices

* Corresponding author: tel: +40 256 491 818
fax: +40 256 491 824, e-mail: *cecilias@acad-icht.tm.edu.ro*

with the possibility of inclusions [1]. Subsequent processing of wet gels, including drying and thermal treatments, is also implicated in structural evolution of sol-gel derived materials.

From phenomenological point of view the process of sol-gel synthesis can be described to be composed from several steps [8,9], such as: i) formation of primary particles as a result of hydrolysis and condensation reactions; ii) primary particle aggregation and formation of clusters, oligomers respectively; iii) clusters aggregation process resulting in larger particles, aggregates, mixtures of polymers with variable sizes; iv) wet gel formation, which can be considered as huge unique solid polymer (occupying the same volume as the initial sol) having pores filled with liquid phase; v) obtaining of the dry gel by elimination of the liquid phase by drying; and finally, vi) thermal treatment of dried gels.

Porosity and grain size generation in nanometer scales is a crucial factor for most of applications and the sol-gel method appeared to be particularly attractive to achieve these objectives. The use of a porous inorganic matrix provides spatially localized sites for nucleation and minimizes the degree of aggregation of certain particles. In order to obtain the desired properties of synthesized material, the optimum synthesis conditions should be found.

By subjecting a sol gel reaction mixture to the action of high power ultrasound it is possible to promote the hydrolysis and condensation of an alkoxide precursor in water, without using a mutual solvent [10,11]. Tarasevich et al. [12] reported the first observation of the TEOS/water mixture reaction under the action of high power ultrasound in 1984. He described the process which results into an intense increase of the temperature with release of alcoholic vapors. He obtained a homogeneous and transparent solution in a few minutes. Afterwards, Zarzycki's group in France began intensive work to establish the consequence of ultrasonic influence on the textural characteristics of the so-called "sonogels". Esquivias' group used sonogels as matrices to encapsulate semiconductors [13,14].

High energy ultrasonic activation has relevant effects on the chemical reactions because of cavitation phenomena [15,16]. The cavitations generated in ultrasonic (US) field lead to formation of free radicals, breaking down the polymeric long chains and a very efficient mixing of all species present in solution. All these processes promote the polycondensation process along with hydrolysis reactions. Such produced sonicated gels are more branched and have certain similarities with microstructures derived from base catalyzed sol-gel process [11,18,19]. Under sonication, the motion of monomers and clusters is significantly enhanced by cavitations and their collisions can be more effective due to the energy supplied by the cavitations. Varying the conditions, a wide variety of structures can be obtained, from fractals to networks with smooth surfaces [11].

The upper limit for the energy supply corresponds to the dose for which the liquid gels are reacting in situ, in the container during sonication. The actual values for these limits are strongly dependent on the cavitation intensity reached and can be modified by varying the reacting system and conditions [9]. The effective energy, transferred inside to the reaction system, especially when using an ultrasonic bath, is very difficult to evaluate exactly. The experimental setup used in the present study involved an ultrasonic bath. In this case a relatively low ultrasonic intensity can be supplied to the reactants. Consequently, the resulting samples might not offer characteristic features of the so-called "sonogel" [11]. The objectives of the present work were to obtain mesoporous silica matrices by sol-gel synthesis, in which TEOS was hydrolyzed in hydro-alcoholic solution, assisted and non-assisted by an ultrasonic field. Nitrogen adsorption and small-angle neutron scattering (SANS) techniques were used in order to characterize the resulted dry gels microstructure and texture.

II. Experimental

2.1. Sample preparation

Starting from a mixture of tetraethoxysilane (98%) (TEOS) and a hydro alcoholic solution (ethyl alcohol 95% p.a. and distilled water) one huge sample have been prepared. The reactants mixture contained TEOS : C_2H_5OH : H_2O = 1 : 4 : 10 molar ratio and HNO_3 (0.03 mol) as catalyst. All chemicals were commercially available reagent grade products and were used without further purification. The reaction mixture was stirred for 2 hours. Then the homogenized sol volume was divided in 4 samples. One of them, denoted as V103, was sealed in a covered vessel to gel. The other three samples were activated in ultrasonic bath, at different durations: 120 minutes (V103-2 sample), 240 minutes (V103-4 sample), and 360 minutes (V103-6 sample). The ultrasonic activation was realized at constant temperature of about 23°C. The sonicated samples were also sealed to gel at room temperature. After gelation all samples were dried at 60°C, in a laboratory oven, for 48 hours. The dried gels were finaly grinded.

A Cole Parmer 18001 Ultrasonic Cleaning Bath was used, having input power of 180W and output power of 80W at 56 KHz. The water volume in the bath was 1780 ml. The supplied energy relative to bath water content volume can be evaluated as ~ 320 J/cm^3 for 2 hours, ~ 640 J/cm^3 for 4 hours and ~ 960 J/cm^3 for 6 hours sonication duration. We are not sure about the efficiency of the energy transfer from US bath to inside of each sample (50 ml of sol), therefore these values should be considered as relative and approximate only.

2.2. Structural characterization

Textural properties of dried gels were determined by using a BET Analyzer COULTER SA 3100. The measured samples (0.2 g) were warmed at 120°C in vacuum

for 24 hours in order to eliminate the adsorbed species. Nitrogen adsorption-desorption curves were registered at liquid nitrogen temperature of 77 K. The SANS experiment was performed at the Budapest Research Reactor [19,20]. Samples were measured at room temperature.

III. Results and discussion

3.1. Surface area and porosity

The specific surface areas of the samples were calculated using the multiple-point Brunauer-Emmett-Teller (BET) method. The pore size distribution curves were computed by using the Barrett-Joyner-Halenda (BJH) method and pore sizes were obtained from the peak positions of the distribution curves. In Table 1 the main texture features derived from BET measurements are collected.

Adsorption-desorption isotherms for the sonicated (V103-2, V103-4, V103-6 samples) and the reference silica gel (V103) are presented in Fig. 1. Nitrogen adsorption isotherms of IV type, characteristic for mesoporous materials according to BDDT classification [21] were observed for all synthesized samples. A sharp increase in the adsorbed volume of nitrogen due to the capillary condensation was observed only for the sample V103-2 at p/p_0 value slightly smaller than 0.5. This could indicate that the pore size of the material should be rather small since the p/p_0 position of the inflexion point is related to the pore size according to Kelvin equation [22]. The sharpness of the adsorption branches is indicative of a narrow mesopore size distribution. In the case of V103 and V103-4 samples the increase in the adsorbed volumes of nitrogen are rather smooth, which can be a sign of a broad pore size distribution.

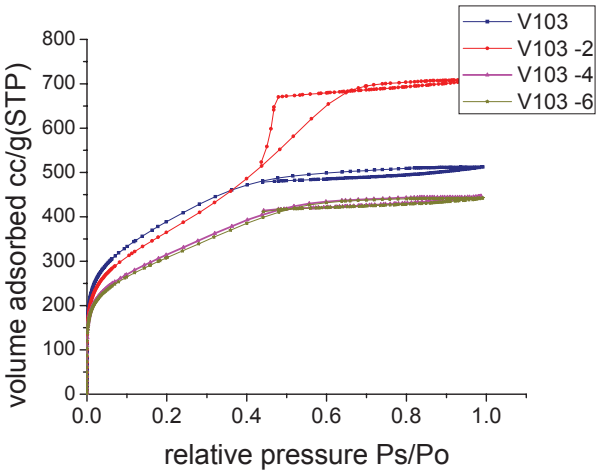

Figure 1. Adsorption-desorption isotherms

The inflexion point corresponds to similar values like in the above mentioned case, but the end of the loop is marked at much larger values of p/p_0, which can indicate the presence of larger pores in these materials.

The adsorption branch for the 2 hours sonicated sample was located at relative pressures in the range of 0.45 to 0.65, and a narrow pore distribution of 90.4% pores up to 60 Å was obtained from BJH desorption method. This material has a BET surface area of 1320 m^2/g and a pore volume of 1.0986 cm^3/g. The BJH adsorption branch gave 88.2% pore size distribution corresponding to the same range with maximum pore size of 60 Å.

In the case of the nonsonicated samples and of those sonicated more than two hours, the adsorption or desorption branches gave different pore size distributions and pore volumes, as shown in Table 2 and Fig. 2. Sil-

Table 1. BET texture characteristics

Sample	BET surface area [m^2/g]	Total pore volume [cm^3/g]	Micropore volume [cm^3/g]	Micropore surface area [cm^3/g]
V103	1404	0.792	0.0610	168.2
V103-2	1320	1.098	0.0116	50.2
V103-4	1129	0.690	0.0558	144.5
V103-6	1105	0.683	0.0545	140.2

Table 2. Pore volume distribution

Pore diameters [nm]	Pore volume distribution [%]							
	V103		V103-2		V103-4		V103-6	
	Desorption	Adsorption	Desorption	Adsorption	Desorption	Adsorption	Desorption	Adsorption
under 6	31.9	72.4	90.4	88.2	37.6	83.6	47.6	89.0
6 – 8	11.0	12.6	2.3	7.6	11.8	6.9	9.7	5.9
8 – 10	6.4	5.0	1.0	1.1	6.4	3.1	5.1	2.2
10 – 12	8.0	4.7	1.1	1.0	7.0	2.3	5.7	1.6
12 – 16	8.63	1.8	1.2	0.9	7.9	0.5	5.3	0.8
16 – 20	8.9	2.1	1.0	0.4	6.9	0.0	7.8	0.3
20 – 80	21.0	1.2	2.3	0.7	16.7	1.7	14.4	0.2
over 80	4.1	0.2	0.7	0.2	5.8	2.0	4.3	0.1

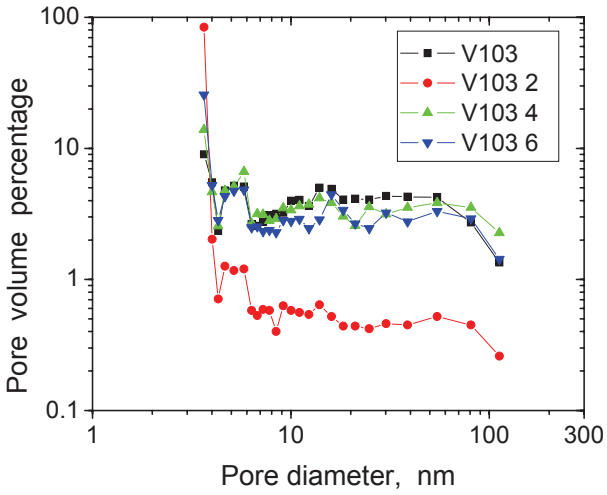

Figure 2. Pore size distribution from BHJ analysis of the desorption isotherms

ica polymeric networks often have roughly spherical pores. Often these pores have "ink bottle" shape, so that spherical bottles are connected to each other by smaller "necks" [23]. In such case, the pore diameter from adsorption reflects the size of the bottle, and the pore diameter from desorption can be associated with the necks between pores [23].

Samples V103 and V103-4 and V103-6 have a relatively broad pore size distribution, indicating that the microstructure of these samples is rather disordered. The reduction of ordered structure of the samples is expressed by the adsorption branches which are located between relative pressures of ~ 0.45–0.92, a wider range compared to that of the more ordered V103-2 sample. The obtained texture properties (total pore volume, micropore volume and micropore surface area) are collected in Table 1.

Among the investigated samples, the V103-2 sample exhibits the lowest micropore volume. The three other samples have much higher microporosity area (three times higher than that of V103-2).

All these observations indicate that the sample sonicated for 2 hours is more ordered: the pore size distribution has a high maximum for small pores, the average size of the pores is lower and the pore shape is closer to a sphere, comparing with the other analyzed samples.

3.2 Small-angle neutron scattering

Small-angle scattering is caused by the inhomogeneous distribution of the material in the investigated sample volume. In our case, this inhomogeneity is related to the non-uniform distribution of the silica material and the pores, occurring on length scales 1–100 nm. The SANS measurements on the four dry gel powders samples have been performed on the conventional SANS diffractometer operating at the cold neutron beamline of the Budapest Research Reactor [19,20]. The data are depicted in the form of the scattered intensity in the function of the magnitude of the scattering vector q. The scattering intensity has been registered over a q range 0.003–0.4 Å^{-1}, using two samples-to-detector distances and two incident wavelengths, 4 Å and 12 Å.

All samples display qualitatively similar scattering curves, which exhibit three characteristic regions. At the lowest q, between 0.003 and 0.01 Å^{-1}, the scattered intensity has a power low behaviour, which shows up as straight line in the double logarithmic presentation (Fig. 3). For the intermediate q, approximately between 0.01 and 0.08 Å^{-1}, a plateau is seen, which is followed by another decay in the high q range, up to 0.45 Å^{-1} (Fig. 4). Such complex shape of the scattering curves indicates that different spatial structures are seen at different magnifications. The quantitative analysis of the experimental data was performed using some frequently used methods applicable for powder and gel-like systems.

High q region The highest q region of the scattering curves corresponds to the smallest measured length scales, for our experimental q range this was in the order of 1–5 nanometers. The gelation process starts with the formation of the so-called primary structural units. They can be considered as spheres having a rough sur-

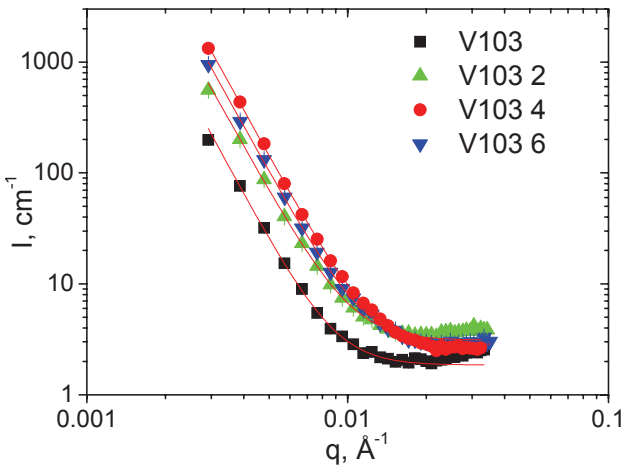

Figure 3. SANS scattering data measured at low q (symbols), and the corresponding power law fits (lines)

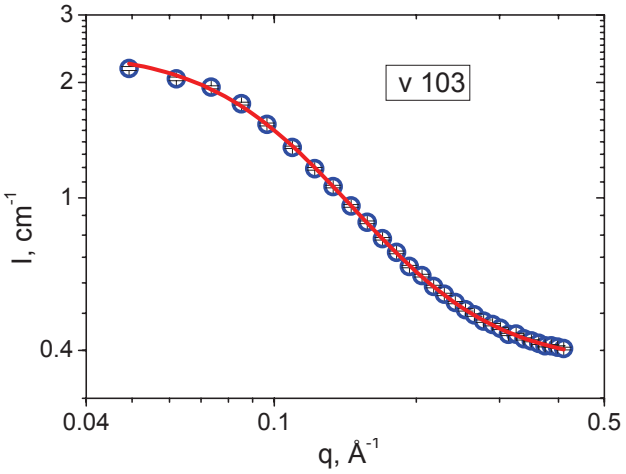

Figure 4. High q part of $I(q)$ data for the sample V103, fitted with the Posselt model

face. The corresponding model, proposed by Posselt [24], equation (1), was applied to the high q part of the measured scattering data and resulted in very good fits for all samples, as shown in Fig. 4. Here r is the nominal radius of the spheres, and Ds is the surface fractal dimension, characterizing the roughness of the surface. The obtained parameters are collected in Table 3.

$$I(q)=\frac{B}{1+0.22(q^2r^2)^{(6-Ds)}}+bg \qquad (1)$$

Low q region The lowest q part of the scattering curves reflects the structure at large size, roughly corresponding to 20–100 nanometers. At this size range, the gels exhibit a power law scattering, described and fitted by equation (2), with power exponents p ranging from 4.2 and 4.4 (collected in Table 3).

$$I(q)=\frac{A}{q^p}+bg \qquad (2)$$

This indicates a complex structure, which cannot be described by either surface or volume fractal, often used for characterization of dry gel materials. In case of pure fractal structure, the power exponent should be less than 4, and $p = 4$ would correspond to a two-phase system (e.g. porous material) with smooth interfaces. It has been shown [25] that $p > 4$ can reflect the situation of a two phase system as well, but the interface must have a gradual change of the density in the direction perpendicular to it. This is also similar to a two-phase system with a rough but non-fractal interface. In our case of dry silica gels, the scattering originates from the plausibly rough interfaces of the porous network of the aggregated primary structural units. The power exponents, as determined by least squares fitting of equation (2), are listed in Table 3. The absolute integrated intensities (accounted for by the prefactor A) are proportional to the amount of the surfaces per unit volume. The internal surface of all samples with received ultrasonic treatment shows increase by an order of magnitude compared to the non-treated sample. In this series, the 4 hours treated sample exhibit the largest surface. It should be noted, that unlike the gas adsorption techniques, the scattering measurement is equally sensitive to the surface of both the closed and the open pores. Unfortunately, without additional and precise knowledge of the pore structure, it is not possible to compare directly the surface and volume characteristics obtained from the two different techniques, even though they are closely related to each other.

IV. Discussion

Structural analysis of the dry gel samples pointed to the nonmonotonic dependence of the gel structure (pore size distribution) on the total applied power. Nitrogen adsorption indicated that the sample sonicated for two hours had a significantly different porosity distribution, than the other three samples. About 90% of the pores have an average dimension of about 3 nm, the fraction of microporosity ($d < 2$ nm) and macroporosity ($d > 50$ nm) being insignificant comparing to the same data of the other samples. Thus, for the given conditions, the duration of the sonication had an optimum value of 2 hours. Concerning the shape of the pores, all samples, except the 2 hours sonicated one, exhibited a rather large difference between the porosity characteristics obtained from the adsorption and desorption branches of the nitrogen adsorption isotherms. Such difference is known to be related to the pore shape, actually to the ink bottle real shape of the pores. For the 2 hours activated sample both branches gave similar porosity data, suggesting that in this case the pore shape is closer to spherical and the microstructure is more ordered compared with the others.

The SANS results reveal the two-level complex structure of the gels. The characteristic size of the primary structural units were found to be 1.5–2 nm, while the secondary porous structure of the aggregated primary units is seen for sizes above 20 nm. The sonication has a strong effect on developing the secondary structure level that is the assembly of the primary quasi-spherical units. The total surface in that size range is by an order of magnitude larger than that of the nonsonicated gel.

V. Conclusions

Altogether four silica matrix samples have been prepared using sol-gel processing, activated by sonication in an ultrasonic bath. The sample texture and microstructure characterization can be resumed in few considerations. Sensible differences were observed among the samples in their texture. As all four samples were prepared by using the same compositional and processing parameters, but different duration of sonication, it could be inferred that the observed changes of

Table 3. SANS parameter values determined by least squares fitting of equations 1 and 2 (all significant digits are given)

Sample	Power exponent p	Low q intensity factor A	High q intensity factor B	Radius [Å]	Ds
V103	4.35	2.4	2.05	15.5	4.50
V103-2	4.21	14.0	2.11	18.4	4.37
V103-4	4.28	20.1	2.07	14.4	4.37
V103-6	4.25	17.1	2.41	15.9	4.43

their properties could be attributed to this variable. The sample sonicated for 2 hours had the best mesoporosity properties, such as the most ordered structure, the lowest average pore size and the most narrow pore size distribution. Due to the low power of the ultrasonic bath, these samples were not classical sonogels as they are defined in literature [11]. By using a simple, low energy consuming methodology we obtained mesoporous materials having huge specific surface areas. They can be useful as matrices for guest materials which require separation, limitation of crystalline growth or preventing aggregation.

Acknowledgements: Experiments in Budapest Neutron Centre were performed with financial support of EC in the framework of the contract no: HII3-CT-2003-505925. The support of COST Program, Action 539 "ELENA" is gratefully acknowledged. C.S. thanks the support of the exchange program between the Hungarian and Romanian Academies, and the DOMUS fellowship.

References

1. C.J. Brinker, G.W. Scherer, *Sol-Gel Science*, Academic Press, San Diego, 1990.
2. L.C. Klein, *Sol-Gel Technology for Thin Films, Fibers, Preforms, Electronics and Specialty Shapes*, Elsevier, NY USA, 1988.
3. R. Aelion, A. Loebel, F. Eirich, "Hydrolysis of ethyl silicate", *J. Am. Chem. Soc*., **72** (1950) 5705–5712.
4. C.J. Brinker, K.D. Keefer, D.W. Schaeffer, R.A.Q. Assink, B.D. Kay, C.S. Ashley, "Sol-gel transition in simple silicates II", *J. Non-Cryst. Solids,* **63** (1984) 45–59.
5. R.J.P. Corriu, "The control of nanostructured solids: A challenge for molecular chemistry", *Eur. J. Inorg. Chem.*, **5** (2001) 1109–1121.
6. G. Cerveau, R. Corriu, C. Lepeytre, "Synthesis of monophasic hybrid organic-Inorganic solids containing [η6-(organosilyl)arene]chromium tricarbonyl moieties" *Chem. Mater*., **9** (1997) 2561–2566.
7. G. Cerveau, R. Corriu, E. Framery, **"**Sol-gel process: Temperature effect on textural properties of a monophasic hybrid material", *Chem. Commun.*, **20** (1999) 2081–2082.
8. R.K. Iler, *Chemistry of Silica*, Wiley, New York, 1979.
9. C.J. Brinker, R. Sehgal, S.L. Hietala, R. Deshpante, D.M. Smith, D. Loy, C.S. Ashley, **"**Sol-gel strategies for controlled porosity inorganic materials", *J. Membrane Sci.*, **94** (1994) 85–102.
10. J. Zarzycki, "Sonogels", *Heterogeneous Chemistry Reviews*, **1** (1994) 243–253.
11. E. Blanco, L. Esquivias, R. Litran, M. Piñero, M. Ramírez-del-Solar, N. de la Rosa-Fox, "Sonogels and Derived Materials", *Appl. Organomet. Chem*., **13** (1999) 399-418.
12. Q. Chen, C. Boothroyd, G.H. Tan, N. Sutanto, A. Mcintosh Soutar, X.T. Zeng, "Silica coating of nanoparticles by the sonogel process", *Langmuir*, **24** (2008) 650–653.
13. M.R. del Solar, L. Esquivias, "Ultrastructural evolution during sintering of mixed sonogels", *J. Sol-Gel Sci. Technol*., **3** (1994) 41–46.
14. L. Esquivias, J. Zarzycki, "Sonogel alternate method", pp. 255–270 in *Proceedings of Sol-Gel Processing in Ultrastructure Processing of Ceramics, Glasses and Composites*. Eds. J.D. Mackenzie, D.R. Ulrich, Wiley, NY, 1988.
15. J.P. Lorimer, T.J. Mason, "Sonochemistry Part 1 − The physical aspect", *Chem. Soc. Rev.*, **16** (1987) 239–274.
16. K.S. Suslick, S.E. Skrabalak, "Sonocatalysis*"* pp. 2007–2017 in *Handbook of Heterogeneous Catalysis*; Eds. G. Ertl, H. Knozinger, J. Weitkamp, Wiley-VCH: Weinheim, 2008.
17. N. de la Rosa-Fox, L. Esquivias, J. Zarzycki, "Glasses from sonogels", *Diffusion and Defect Forum*, **53-54** (1987) 363–374.
18. D.R. Vollet, D.A. Donatti, A. Ibanez Ruiz, W.C. de Castro, "Structural evolution of aerogels prepared from TEOS sono-hydrolysis upon heat treatment up to 1100ºC", *J. Non-Cryst. Solids,* **332** (2003) 73–79.
19. L. Rosta, "Cold neutron research facility at the Budapest Neutron Centre", *Appl. Phys. A*, **74** (2002) S52–S54.
20. L. Cser, L. Rosta, Gy. Török, "Neutron scattering facilities at Budapest's modernized reactor*, Neutron News*, **4** [2] (1993) 9–15.
21. IUPAC Recommendations, *Pure Appl. Chem*., **66,** (1994) 1739–1758.
22. J.M. Haynes, "Pore size analysis according to the Kelvin equation", *Mater. Struct*. **6** (1973) 209–213.
23. M. Thommes, B. Smarsly, M. Groenewolt, P. Ravikovitch, A. Neimark, "Adsorption hysteresis of nitrogen and argon in pore networks and characterization of novel micro- and mesoporous Silicas", *Langmuir*, **22**, (2006) 756–764
24. D. Posselt, J.S. Pedersen, K. Mortensen, "A SANS Investigation on Absolute Scale of a Homologous Series of Base-Catalysed Silica Aerogels", *J. Non-Cryst. Solids*, **145** (1992), 128–132.
25. P.W. Schmidt, "Some fundamental concepts and techniques useful in small-angle scattering studies of disordered solids" *in Modern aspects of small-angle scattering*, ed. by H. Brumberger, Kluwer Academic Publishers, Netherlands, 1995.